4th International Conference on High-Performance Marine Vehicles
Rome, 27-29 September 2004

Numerical Models of Water Impact

Hajime Kihara, National Defense Academy, Japan, hkihara@nda.ac.jp

Abstract

This paper presents a numerical method for studying water impact of a two-dimensional body of arbitrary cross-section. The global simulation procedure based on the boundary element method is constructed. The attention is focused on the computational description of the jet flow in the framework of a potential flow assumption. The proposed computational model makes the numerical analysis more stable, in addition, enables the simulation of the flow deformation due to the gravity effect. Water impact problems due to the vertical impulsive motion of an initially floating body are considered. The prediction of hydrodynamic pressure is found to be in good agreement with similarity solutions for wedges with different dead-rise angle.

1 Introduction

Water impact is one of the critical phenomena from a viewpoint of the structural design of ships or offshore structures. Since the further development of von Karman's theory was made by Wagner (1932), considerable attention has been turned to broad studies on the water impact problems. The similarity solutions for a two-dimensional wedge were first obtained by Dobrovol'skaya (1969), which were the complete ones based on the nonlinear theory. The jet flow is generated due to the impulsive motion of a floating body or the water entry of a body. It is one of characteristic features in water impact phenomena. The theoretical approach using asymptotic expansions can recover the effect of the jet flow, which was made by, for example, Armond and Cointe (1987), Howison et al. (1991), Chapman et al. (1997), Faltinsen (2002), and Iafrati and Korobkin (2002). As related works, the compressibility of the fluid in a moment of impact was discussed by Korobkin (1996)(2004). On the other hand, the numerical approach by the boundary element method (BEM) is also one of practical procedures in which the jet region can be taken into account. However, it is well-known that the velocity is singular at an intersection between the body and the free surface. The ordinary computation often gives rise to some problems on the accuracy or the stability of solutions. Accordingly, it is one of challenging issues how the jet flow is dealt with in computation.

Zhao & Faltinsen (1993) proposed the so-called "cut-off" model, in which a new computational segment is introduced at the jet root position and the upper part of the jet region is removed from the computation. This model provides so good prediction of the hydrodynamic pressure on wedges with various deadrise angles that it is adopted in the studies by Lu et al. (2000) and Battistin and Iafrati (2003). This operation is very practical from an engineering viewpoint, because the hydrodynamic pressure on the body in the jet region is almost equal to atmospheric one. As studies with the similar concept where the jet flow was ignored, the practical method based on the generalized Wagner theory was presented by Zhao & Faltinsen (1996) and Mei et al. (1999). However, as the jet flow is cut off at the spray root, we cannot obtain the information, for instance, the evolution of the jet flow and the separation from the body surface. Recently the interesting method that can make up with the drawback of the model was presented by Battistin and Iafrati (2004). The jet region is divided into several small panels and the velocity potential on each panel is computed by using local Taylor expansions and matching with the other domain.

The present study is intended to develop the numerical procedures by the BEM, by which we can describe the evolution of the jet flow in the water impact as well as the prediction of the hydrodynamic pressure. For this purpose, we introduce a computational model about the jet

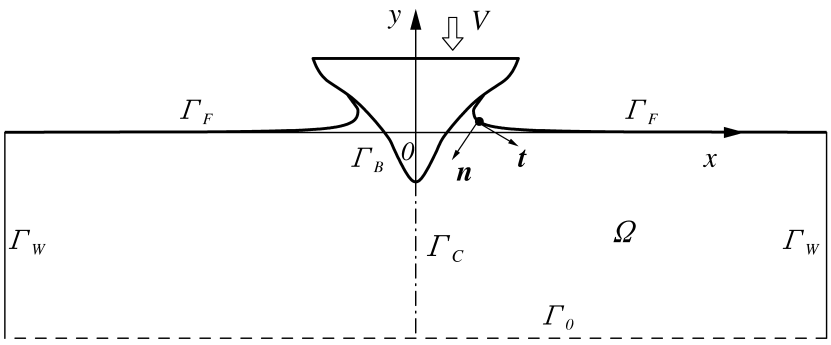

Fig. 1: Definition of coordinate system.

flow. It is regarded as a kind of cut-off models, but the cut-off operation is restricted only to the jet tip in order to keep the computed information. Our idea may be conceptually similar to the model by Fontaine & Cointe (1997), although their computational results near jet tips are different from ours judging from their published results. As we describe this computational model of the jet flow in section 2.3.2, we'd like to emphasize that such a manner is arbitrary to some extent. It suggests that the exact description of the flow is not always necessary within the jet region.

2 Numerical simulation for water impact

2.1 Formulations of problems

We consider the water entry problem of a two-dimensional symmetrical body, in which the initially floating body on the free surface moves down with impulsive vertical motion, that is, abruptly starting motion. The x and y axes are taken along the undisturbed free surface and along the body centerline pointing upward, respectively, as is shown in Fig.1. The water entry velocity $\boldsymbol{v}_B = -V\boldsymbol{e}_y$ is assumed to be constant during the impact, the $\boldsymbol{e}_y$ being the unit vector along the y-axis. The fluid domain Ω is surrounded by boundaries consisting of the free surface Γ_F, the body surface Γ_B, side walls Γ_W, and the bottom Γ_0. Assuming the fluid is incompressible and the flow is irrotational, the fluid motion is specified by the velocity potential ϕ. The problem of the velocity field is governed by the following equations:

$$\nabla^2\phi = 0 \qquad \text{in} \quad \Omega \tag{1}$$

$$\frac{\partial\phi}{\partial n} = \boldsymbol{v}_B \cdot \boldsymbol{n} = -Vn_y \qquad \text{on} \quad \Gamma_B \tag{2}$$

$$\frac{D\phi}{Dt} = \frac{1}{2}|\nabla\phi|^2 - gy \qquad \text{on} \quad \Gamma_F \tag{3}$$

$$\frac{D\boldsymbol{x}}{Dt} = \nabla\phi \qquad \text{on} \quad \Gamma_F \tag{4}$$

$$\frac{\partial\phi}{\partial n} = 0 \qquad \text{on} \quad \Gamma_W,\ \Gamma_0,\ (\Gamma_C) \tag{5}$$

where g is the acceleration of gravity and the position vector of arbitrary point in the domain is expressed by $\boldsymbol{x} = (x, y)$. The gravity term in equation (3) is retained for the realistic description of the problem, while it is neglected in ordinary analysis on the water impact because the gravity effect is considered small during the impact.

The hydrodynamic pressure can be computed by using the Bernoulli equation. On that occasion, the time derivative of the velocity potential is necessary. Although it can be obtained by using the finite difference method to the velocity potential, the computational accuracy of the pressure is generally said to be not good. For more accurate prediction, the boundary value problem as for $\partial\phi/\partial t = \phi_t$ is also considered in the present study. The validity of such an approach is demonstrated widely, for example, in results of the ISOPE benchmark test (1999). Such a boundary problem related with the acceleration field can be described as follows:

$$\nabla^2\phi_t = 0 \qquad \text{in} \quad \Omega \tag{6}$$

$$\frac{\partial\phi_t}{\partial n} = \kappa\left|\nabla\phi\right|^2 + \frac{\partial\phi}{\partial n}\frac{\partial^2\phi}{\partial s^2} - \frac{\partial\phi}{\partial s}\frac{\partial}{\partial s}\frac{\partial\phi}{\partial n} \qquad \text{on} \quad \Gamma_B \tag{7}$$

$$\phi_t = -\frac{1}{2}\left|\nabla\phi\right|^2 - gy \qquad \text{on} \quad \Gamma_F \tag{8}$$

$$\frac{\partial\phi_t}{\partial n} = 0 \qquad \text{on} \quad \Gamma_W,\ \Gamma_0,\ (\Gamma_C) \tag{9}$$

where $\partial\ /\partial s$ is the tangential derivative along the boundary, and κ denotes the local curvature of the body contour. The general form about the normal derivative of ϕ_t on the body in motion was shown by Tanizawa (1995). The condition is simplified to equation (7) for the translational motion with constant velocity. Although the similar conditions are shown by by Cointe et al. (1990), van Daalen (1993) and Wu and Eatock Taylor (1996), these lead to the same condition for a body shape without curvature like a wedge.

The initial conditions of the free surface are necessary to complete the problems. Although the small portion of the body is already submerged into water, there is no initial disturbance on the free surface. Such conditions are given by:

$$\phi = \phi_t = \eta = 0 \qquad \text{on} \quad \Gamma_F \quad \text{at} \quad t = 0 \tag{10}$$

where η denotes the free surface elevation. The treatment of the initial condition is important to discuss the nonlinear wave-body interaction due to the impulsive motion, because the prediction of the hydrodynamic pressure on a body is affected at the early stage of the impact. This point is discussed more in section 2.3.1, and the practical approach to complement such influence is presented in section 4.

Thus the water entry problems of a body are formulated as the initial value - boundary value problems. Considering the symmetrical property of the problem, we can reduce the fluid domain to analyze to half, that is, the fluid domain in $x \geq 0$, where the boundary Γ_C on the y-axis is newly complemented.

2.2 Numerical procedures

2.2.1 Solution procedure of integral equation

Two sets of boundary value problems in equations (1)-(5), (6)-(9) can be solved using the BEM. Applying Green's theorem to the boundary value problems, the integral equations with the same form are derived as follows:

$$C(\boldsymbol{\xi})\begin{Bmatrix}\phi(\boldsymbol{\xi})\\ \phi_t(\boldsymbol{\xi})\end{Bmatrix} + \int_\Gamma \begin{Bmatrix}\phi(\boldsymbol{x})\\ \phi_t(\boldsymbol{x})\end{Bmatrix}\frac{\partial G(\boldsymbol{\xi},\boldsymbol{x})}{\partial n(\boldsymbol{x})}\,d\Gamma(\boldsymbol{x}) = \int_\Gamma \begin{Bmatrix}\phi(\boldsymbol{x})\\ \phi_t(\boldsymbol{x})\end{Bmatrix}\,d\Gamma(\boldsymbol{x}) \tag{11}$$

where $\boldsymbol{\xi}$ and $\boldsymbol{x}$ are an observation point and an integral point, respectively. The free term $C(\boldsymbol{\xi})$ is given by:

$$C(\boldsymbol{\xi}) = -\int_\Gamma \frac{\partial G(\boldsymbol{\xi},\boldsymbol{x})}{\partial n(\boldsymbol{x})}\,d\Gamma(\boldsymbol{x}) \tag{12}$$

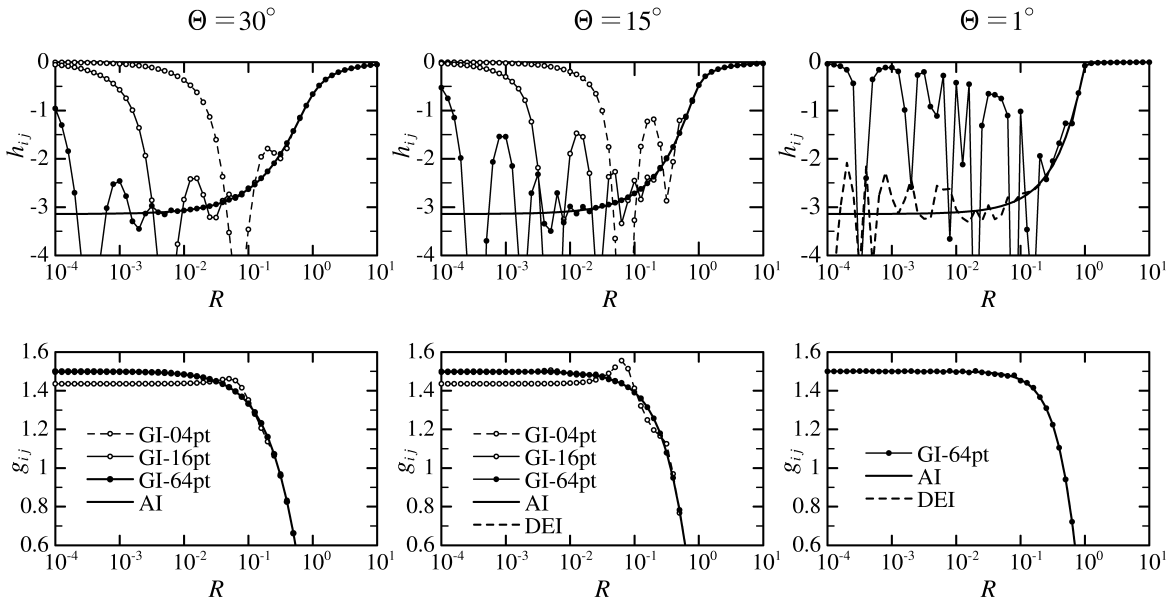

Fig. 2: Evaluation of influence coefficients for the distance R and the angle Θ between $(\boldsymbol{x}_j - \boldsymbol{\xi}_i)$ and $(\boldsymbol{x}_{j+1} - \boldsymbol{x}_{j-1})$, where the internal angle between Γ_j and Γ_{J+1} is π and the length of each element is unity. GI:Gaussian integration, AI:Analytical integration, DEI:Double exponential integration.

The integral contour Γ means the boundary surrounding the fluid domain, that is, $\Gamma = \Gamma_B \cup \Gamma_F \cup \Gamma_W \cup \Gamma_C$. It is noted that the bottom boundary Γ_0 is excluded from computation here. Then the Green function $G(\boldsymbol{\xi}, \boldsymbol{x})$ is expressed by using the source as follows:

$$G(\boldsymbol{\xi}, \boldsymbol{x}) = \frac{1}{2\pi} \ln \frac{1}{|\boldsymbol{x} - \boldsymbol{\xi}|} + \frac{1}{2\pi} \ln \frac{1}{|\boldsymbol{x} - \boldsymbol{\xi}^*|} \tag{13}$$

where $\boldsymbol{\xi}^*$ denotes the image point of $\boldsymbol{\xi}$ about the bottom Γ_0. Additionally, the boundary Γ_C can be excluded from the computation by introducing other source images. However, it doesn't result in the effective reduction of computational time in using the free surface boundary with a long distance.

The linear isoparametric elements are used for the discretization of the boundary Γ in the present study. Adjacent nodes $\boldsymbol{x}_j$ and $\boldsymbol{x}_{j+1}$ connect an element Γ_j, on which the variations of both the geometric shape and the physical quantity, such as the velocity potential, are assumed linear. The influence coefficients can be evaluated by the following equations:

$$h_{ij} = \int_{\Gamma_j} f^{(2)}(l) \frac{-1}{r(l)} \frac{\partial r(l)}{\partial n} d\Gamma(l) + \int_{\Gamma_{j+1}} f^{(1)}(l) \frac{-1}{r(l)} \frac{\partial r(l)}{\partial n} d\Gamma(l) \tag{14}$$

$$g_{ij} = \int_{\Gamma_j} f^{(2)}(l) \ln \frac{1}{r(l)} d\Gamma(l) + \int_{\Gamma_{j+1}} f^{(1)}(l) \ln \frac{1}{r(l)} d\Gamma(l) \tag{15}$$

where $r = |\boldsymbol{x} - \boldsymbol{\xi}_i|$, the variable l is the local coordinate along each element, and $f^{(1)}(l)$ and $f^{(2)}(l)$ are interpolation functions which are given by:

$$f^{(1)}(l) = \frac{1}{2}(1 - l), \quad f^{(2)}(l) = \frac{1}{2}(1 + l), \quad -1 \le l \le 1 \tag{16}$$

The computational accuracy of these integrals is extremely important in the BEM analysis. Some results of the evaluation for equations (14) and (15) are shown in Fig.2. Since we have to deal with the special geometric shape of the jet region in water impact problem, it is guessed that the numerical integration leads to the instability easily. Therefore the analytical integration

is adopted in the present study. When the integrals in equations (11) and (12) are performed on each element, the following matrix equations concerning the velocity potential and its flux can be derived:

$$[H_{ij}]\{\phi_j\} = [G_{ij}]\{\phi_{nj}\} \qquad (i,j = 1,2,\cdots,N) \tag{17}$$

where ϕ_n denotes the normal derivative of the velocity potential and H_{ij} and G_{ij} are the influence coefficients in using equation (13). On the free surface Γ_F, the velocity potential is known and its flux is unknown. On the other hand, the velocity potential is unknown and its flux is known on the other boundaries. Tranforming equation (17) to the simultaneous equations concerning unknowns, we can solve these numerically by using an ordinary scheme for the linear system, such as the Gaussian elimination method. As for ϕ_t and its flux ϕ_{tn}, we can solve in the same manner as the problem for the velocity field. Since the influence coefficients in equation (17) are available in common, it does not lead to increase of large computational loads.

Once the boundary value problem of velocity field is solved at a certain time step, the boundary conditions of the boundary value problem for ϕ_t can be set. Solving two kinds of boundary value problems, we can compute the pressure on a body by:

$$\frac{p}{\rho} = -\frac{\partial\phi}{\partial t} - \frac{1}{2}|\nabla\phi|^2 - gy \tag{18}$$

where ρ is the fluid density. The hydrodynamic loads can be obtained by integrating the pressure over the instantaneous wetted surface of a body.

2.2.2 Time integration procedure

The boundary conditions have to be updated for the computation at next time step. This is achieved by the integration of equations (3) and (4). By using values at the former time step, the position $\boldsymbol{x}_j$ and its velocity potential ϕ_j at the next time step, can be written as:

$$\boldsymbol{x}_j(t+\Delta t) = \boldsymbol{x}_j(t) + \int_t^{t+\Delta t} \left\{ \boldsymbol{t}\frac{\partial\phi(\tau)}{\partial s} + \boldsymbol{n}\frac{\partial\phi(\tau)}{\partial n} \right\} d\tau \tag{19}$$

$$\phi_j(t+\Delta t) = \phi_j(t) + \int_t^{t+\Delta t} \left\{ \frac{1}{2}|\nabla\phi(\tau)|^2 + gy(\tau) \right\} d\tau \tag{20}$$

where $\boldsymbol{t}$ and $\boldsymbol{n}$ denote a tangential and a normal vector, respectively. The tangential derivative of the velocity potential can be computed by using the numerical differentiation:

$$\left.\begin{aligned} \left(\frac{\partial\phi}{\partial s}\right)_j &= \left(\frac{\partial\phi}{\partial j}\right)_j \Big/ \left(\frac{\partial s}{\partial j}\right)_j \\ \left(\frac{\partial x}{\partial s}\right)_j &= \left(\frac{\partial x}{\partial j}\right)_j \Big/ \left(\frac{\partial s}{\partial j}\right)_j \\ \left(\frac{\partial y}{\partial s}\right)_j &= \left(\frac{\partial y}{\partial j}\right)_j \Big/ \left(\frac{\partial s}{\partial j}\right)_j \end{aligned}\right\} \tag{21}$$

where the index j corresponds to the node number of $\boldsymbol{x}_j$, and each term is evaluated using the Lagrange five point interpolation formula. As a time-marching scheme, the fourth-order Runge-Kutta method is employed in the present study. Then the time step size Δt is chosen in consideration of the following condition:

$$\max\{\,|\nabla\phi_1|, |\nabla\phi_2|, \cdots, |\nabla\phi_{N_F}|\,\} \times \Delta t \;\le\; c_s \times \min\{\,\Delta s_1, \Delta s_2, \cdots, \Delta s_{N_F-1}\,\} \tag{22}$$

where $\nabla\phi_j$ and Δs_j are the velocity of a node $\boldsymbol{x}_j$ and the length of an element Γ_j, respectively, and N_F is node numbers of a moving boundary Γ_F. The coefficient c_s is set to 1/3. Since we

encounter the occasion that a time step size is not adequately small, the computational scheme that the time step is automatically divided to smaller one is adopted.

Finally, the control of spatial discretization during computation is indispensable in following fluid particles in a Lagrangian manner. The high resolution is needed to describe small -scale features with high curvature. However, it is not preferable that the node density is too high or too low at the part of moving boundary, because the drop of computational accuracy may lead to the instability, specially in the region where the velocity gradient is so high. The quasi -uniformity condition for node distribution is significantly effective, and it can be formulated as:

$$\frac{\Delta s_{j-1}}{c_u} \leq \Delta s_j \leq c_u \, \Delta s_{j-1} \tag{23}$$

where c_u is a constant sufficiently large than 1 and always set to 3 in the present study.

2.3 Computational model of jet flow

2.3.1 Treatment of the intersection

In the studies of nonlinear wave-body interactions, specially considering the fluid behavior due to abruptly starting motion, the treatment of a wave-body surface intersection has been discussed by Lin et al. (1984), Yim (1985), Greenhow (1987) and Takagi et al. (1989). Summarizing those, the problems are collected to the following two points: (i) Computational accuracy, (ii) Stability of computation. That is, when computational points are increased near the intersection, computational results get closer to the analytical solutions, but the solutions are easy to become unstable. On the other hand, when computational points are decreased near the intersection, a computational scheme becomes hard to be broken down, but the mass or the energy are hard to be conserved. Generally, It is explained that these problems result from the presence of singularities at the intersection.

The first point becomes important at the early stage of water impact. It means that a very high resolution is needed in the computation near the intersection, because the free surface part with high curvature due to the jet is formed within a small time scale. The asymptotic behavior of the fluid at $t \to 0^+$ is studied by Roberts (1987) for the horizontal impulsive motion of a vertical plate, and by Iafrati and Korobkin (2000) for the vertical impulsive motion of a wedge. Korobkin (2004) concludes that the compressibility of the fluid should be taken into account at the early stage of the water impact. It suggests that the initial disturbance should be taken into account in the water impact analysis of the incompressible fluid. In the water impact analysis of a wedge, it is well-known that self-similarity solutions can be obtained in considering the problem in the dimensionless plane, which is called the similarity plane in the present work for simplicity. Especially, we can avoid the above-mentioned resolution problem in this approach, because there is no scale of disturbance changed by time, in principle. Self-similarity solutions for the wedge impact can be obtained using the iterative numerical method by Tanizawa (1985), Ohtsubo and Fukumura (1987), Wu et al.(2004) and Battistin and Iafrati (2004). The similar approach is also studied in the present study, and it is discussed in section 4. The computational scheme is designed for nodes to be arranged intensively near the boundary with high curvature in the present simulation method on the physical plane. Nevertheless we can expect the better results in using the similarity solutions as the initial condition.

The second point in the water impact problem is considered to have close relation to the contact angle which is made between the body and the free surface. The introduction of analytical integration for the influence coefficients ensure stable computation as shown in section 2. Actually even though the contact angle becomes less than 1°, the computation does not break down unless both boundaries touch each other. Therefore, although the substantial cause cannot be

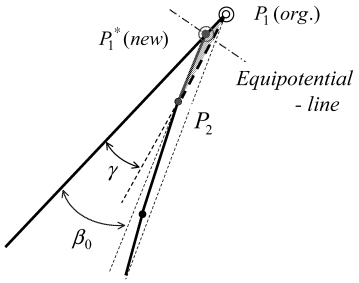

Fig. 3: Cut-off operation of a jet tip.

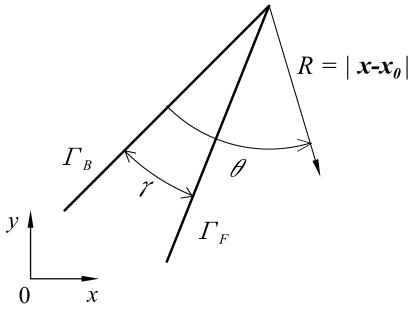

Fig. 4: Local coordinate system.

specified here, we can conclude that the four numerical factors should be evaluated for success computation, which consists of the numerical description of the geometric shape of the moving boundary, the setting of time step size, the control of nodal arrangement and the integration of boundary elements.

2.3.2 Modified cut-off model

The impulsive motion of a body induces very large acceleration near the intersection and then the fluid runs up along the body surface quickly. Theoretically the velocity is singular at the intersection in a moment of the water impact. It means that the velocity is infinite there. However, the computed velocity values based the nonlinear theory are finite, and numerical errors are inherent in the computation of the intersection for the short duration after the water impact. It implies that there is the arbitrariness to a certain extent. Considering actual fluid phenomena on the jet, the fluid is disintegrated into clouds of droplets, which is no longer the continuous fluid domain. We can trace the motion of a jet tip to some extent, but computational efforts will be added more and more because of an increase in a computational domain. At last, such a situation leads to the numerical instabilities bringing the small negative pressure and the contact of boundaries causing the computational break . From the above-mentioned considerations, we introduce the cut-off model to describe the jet flow practically. We assume that the body surface is approximately straight near the intersection. The cut-off operation in a thin triangle layer with an apex at the intersection is illustrated in Fig.3. Since the velocity potential comes to have almost symmetry values on both boundaries, the flow can be considered one-dimensional toward the intersection. The tip shape of the jet region is controlled only by the contact angle γ. The execution of the cut-off operation is judged by the condition:

$$\gamma \leq \beta_0 \quad \text{at} \quad P_2 \tag{24}$$

The shadow area in Fig.3 is removed when the above condition is violated. So the contact angle γ is always monitored during computations. The results by Dobrovol'skaya (1969) are adopted as the threshold angle β_0 in the present work. We expand the velocity potential ϕ in Taylor series around the intersection $\boldsymbol{x}_0$ as follows:

$$\phi(\boldsymbol{x}) = \phi(\boldsymbol{x}_0) + (\boldsymbol{x} - \boldsymbol{x}_0) \cdot \nabla\phi(\boldsymbol{x}_0) + \frac{1}{2!}\left\{(\boldsymbol{x} - \boldsymbol{x}_0) \cdot \nabla\right\}^2 \phi(\boldsymbol{x}_0) + \cdots \tag{25}$$

Two terms in the above equation are considered sufficient to describe the jet flow near the intersection. By the local coordinate system in Fig.4, if the following conditions:

$$\left.\begin{aligned} &\phi(R,0) = \phi(R,\gamma) \\ &\frac{\partial\phi(R,0)}{\partial R} = \frac{\partial\phi(R,\gamma)}{\partial R}, \quad \frac{\partial\phi(R,0)}{R\,\partial\theta} = \frac{\partial\phi(R,\gamma)}{R\,\partial\theta} \end{aligned}\right\} \tag{26}$$

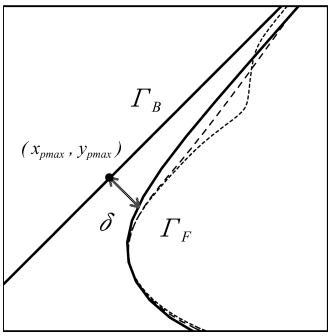

Fig. 5: Sketch near a jet root.

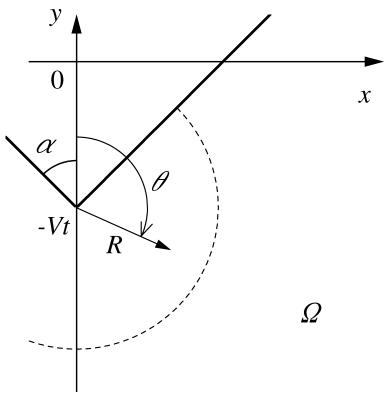

Fig. 6: Sketch around a bottom apex.

are approximately satisfied closely near the intersection, the mass and energy conservation are within the acceptable range even in cutting off the jet tip.

2.4 Matching of analytical solutions for a bottom singularity

In the water impact of a body with a sharp apex at the bottom, such as a wedge, we need to pay attention to the presence of a singularity at the apex, as pointed out by Yim (1987). It turned out that the prediction of the local hydrodynamic pressure around the apex was subject to be affected by computational errors. It is more remarkable as the apex angle becomes small. In the numerical approach, the shift of a source point inside from the apex brings some improvements, for example, by using a constant element or a non-conformity element as the element adjacent to the apex. However, it still remain the influence of the numerical differentiation, the type of its scheme and the choice of nodal intervals. Therefore, to reduce such disadvantage, the analytical expression of velocity potential is adopted in the local domain around the apex, as shown in Fig.6. Such analytical solutions are expressed as:

$$\phi = V \sum_{m=1}^{M} a_m R^{\frac{(m-1)\pi}{\pi-\alpha}} \cos\left\{\frac{(m-1)(\theta-\alpha)\pi}{\pi-\alpha}\right\} - VR\cos\theta \tag{27}$$

where a_m is a coefficient to be determined by matching with the solutions in the other domain. Equation (27) satisfies both the Laplace equation and the body boundary condition. The discretized form can be written as:

$$\{\phi_k\} = [F_{km}]\{a_m\} + \{b_k\} \qquad (k, m = 1, 2, \cdots, M < N) \tag{28}$$

The matrix and vector of right-hand side are given by

$$\begin{cases} F_{km} = VR_k^{\sigma_m} \cos\{\sigma_m(\theta-\alpha)\}, \quad \sigma_m = \dfrac{(m-1)\pi}{\pi-\alpha} \\ b_k = VR_k\cos\theta \end{cases} \tag{29}$$

Let the local boundary (M nodes) locate in the first half of the total boundary (N nodes). Substituting equation (29) to the left-hand side of (17), the matrix form is

$$\left[\begin{array}{c|c} H_{ik} & H_{il} \end{array}\right] \left\{\begin{array}{c} \phi_k \\ \hline \phi_l \end{array}\right\} = \left[\begin{array}{c|c} H^*_{im} & H_{il} \end{array}\right] \left\{\begin{array}{c} a_m \\ \hline \phi_l \end{array}\right\} + \left\{\begin{array}{c} b^*_i \end{array}\right\} \tag{30}$$

The new matrix and vector with the symbol* can be computed by

$$[H^*_{im}] = [H_{ik}][F_{km}] \tag{31}$$

$$\{b^*_i\} = [H_{ik}]\{b_k\} \tag{32}$$

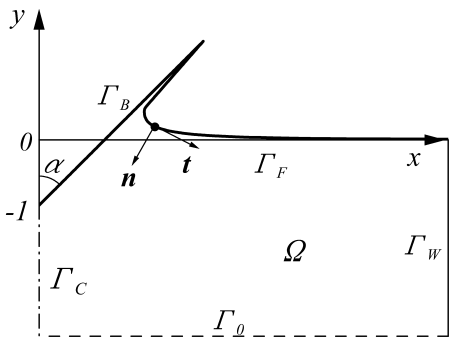

Fig. 7: Definition of coordinate system.

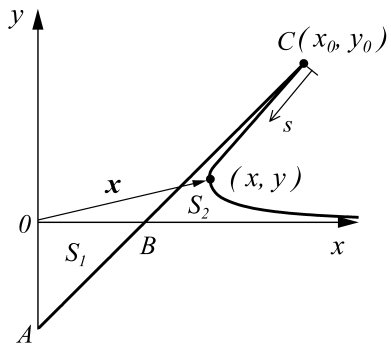

Fig. 8: Sketch of self-similarity flow.

The total number of unknowns is the same as that before introducing equation (27). Therefore, using equation (30), we can solve the simultaneous equations with unknown coefficients a_m matched with the velocity potential ϕ_l in the remaining domain. In the present work, the radius distance of the local domain is set to $Vt/2$.

3 Similarity solutions of wedge impact problem

3.1 Formulation of the problem

We studies the wedge impact problem here by following two reasons. One is for purposes of comparison with the computational results by the nonlinear simulation method, and the other is for the use of similarity solutions as initial conditions in the nonlinear simulation method. This concept is based on the assumption that these similarity solutions are applicable as initial conditions in spite of the arbitrary-shaped body.

We consider the water impact problem for a symmetrical wedge with half apex angle α. When the velocity V is constant and the gravity is neglected, the solution is self-similar and the independent variables $\bar{\boldsymbol{x}}$ and t are reduced to a dimensionless variable $\boldsymbol{x}$ defined by:

$$\boldsymbol{x} = \frac{\bar{\boldsymbol{x}}}{Vt} \tag{33}$$

The velocity potential $\bar{\phi}$ in the physical plane is related to the dimensionless one ϕ defined by:

$$\phi = \frac{\bar{\phi}}{V^2 t} \tag{34}$$

By using these variables, the boundary value problem (1)-(5) can be rewritten as follows:

$$\nabla^2 \phi = 0 \qquad \text{in} \quad \Omega \tag{35}$$

$$\frac{\partial \phi}{\partial n} = \boldsymbol{v}_B \cdot \boldsymbol{n} = -n_y = \sin\alpha \qquad \text{on} \quad \Gamma_B \tag{36}$$

$$\phi - \boldsymbol{x} \cdot \nabla\phi + \frac{1}{2}|\nabla\phi|^2 = 0 \qquad \text{on} \quad \Gamma_F \tag{37}$$

$$\frac{\partial \phi}{\partial n} = \boldsymbol{n} \cdot \boldsymbol{x} \qquad \text{on} \quad \Gamma_F \tag{38}$$

$$\frac{\partial \phi}{\partial n} = 0 \qquad \text{on} \quad \Gamma_W,\ \Gamma_0,\ (\Gamma_C) \tag{39}$$

where $\boldsymbol{v}_B$ is dimensionless velocity of a wedge and equal to $-\boldsymbol{e}_y$ in the present case. The problem is illustrated in Fig.7. The kinematic free surface condition (38) provides

$$\nabla\phi = \boldsymbol{x} - s\boldsymbol{t} \quad (s \geq 0) \qquad \text{on} \quad \Gamma_F \tag{40}$$

where s is the parameter along the free surface as shown in Fig.8. The gradient of the dynamic free surface condition (37) gives $-(\boldsymbol{x}\cdot\nabla)\phi+(\nabla\phi\cdot\nabla)\nabla\phi=0$, in addition, by the substitute of equation (40) and the consideration that the gradient of s means the tangential vector, the sign of the second term in equation (40) can be decided as the negative. When $s=0$, it corresponds to the intersection $\boldsymbol{x}_0$. Taking the scalar product of equation (40) with $\boldsymbol{t}$, the tangential velocity on the free surface is given by:

$$\frac{\partial\phi}{\partial s}=\boldsymbol{t}\cdot\boldsymbol{x}-s \qquad \text{on} \quad \Gamma_F \tag{41}$$

Substituting equation (40) to the dynamic condition (37), the velocity potential can be written by:

$$\phi=\frac{1}{2}(\,|\boldsymbol{x}|^2-s^2\,)=\frac{1}{2}(\,r^2-s^2\,) \qquad \text{on} \quad \Gamma_F \tag{42}$$

where $r=|\boldsymbol{x}|=\sqrt{x^2+y^2}$. The above equation can be also derived from integrating equation (41) in s. It should be noted that equations (40), (41) and (42) are respectively derived from the combination of both free surface conditions (37) and (38).

From thr above-mentioned consideration, the problem can be formulated as the Neumann boundary value problem: (35), (36), (38) and (39), or the mixed boundary value problem: (35), (36), (39) and (42), alternatively. More careful treatment is necessary in the Neumann problem as referred to in the next section.

3.2 Numerical procedures by iterative computations

For the mixed boundary problem, the solution procedure by the boundary integral equation is available, which is already presented in section 2.2.1. Initially the free surface shape being given, the similarity solutions are computed by the iterative procedures until the solutions converge. On the other hand, for the Neumann problem, an additional condition is indispensable for the uniqueness of solutions, which is complemented by giving the ϕ on a point on the boundary. For example, we can do so by using equation (42) to the intersection. However, the position of the intersection sensitively affect the velocity potential ϕ on the body surface, and more careful treatment is necessary in judging the convergence of computations. Therefore, we recommend dealing with the mixed problem.

It should be noted that there are no physical meanings in the computation on the similarity plane under iterative process. We employ the following solution as the initial free surface shape.

$$y=\frac{x}{c}\sin^{-1}\left(\frac{c}{x}\right)-1, \quad x\geq c \tag{43}$$

where $c=(\pi/2)\tan\alpha$. The modification of the free surface shape is performed in the similar manner to the time-stepping scheme as follows:

$$\boldsymbol{x}_j(t+\Delta t)=\boldsymbol{x}_j(t)+\int_t^{t+\Delta t}\boldsymbol{t}\frac{\partial\phi(\tau)}{\partial s}\,d\tau \tag{44}$$

where Δt is a quasi-time step size and not sensitive to the computation. The integrand can be computed using equation (41). In these steps, with the nodes shifted, the shape is modified in order to satisfy the free surface condition. The slip condition is imposed on the intersection along the body surface. When the convergence is achieved to some extent, the following equation

$$\boldsymbol{x}_j(t+\Delta t)=\boldsymbol{x}_j(t)+\int_t^{t+\Delta t}\left(\frac{\partial\phi(\tau)}{\partial n}-\boldsymbol{n}\cdot\boldsymbol{x}\right)d\tau \tag{45}$$

is employed in order to satisfy the kinematic condition much more. Every time the free surface is updated, the velocity potential on it can be computed from equation (42).

As for the treatment of the jet flow, the cut-off method in section 2.3.2 can be applied. However, we are not interested in the free surface deformation due to the gravity effect here, and cut off it at the jet root position $\boldsymbol{x}$ on the free surface. Substituting $\nabla\phi(\boldsymbol{x}_0) = \boldsymbol{x}_0$ to the two term expansions in (25), we obtain

$$\begin{aligned} \phi(\boldsymbol{x}) &= \phi(\boldsymbol{x}_0) + (\boldsymbol{x} - \boldsymbol{x}_0)\cdot\boldsymbol{x}_0 \\ &= \frac{1}{2}\left\{ |\boldsymbol{x}|^2 - |\boldsymbol{x} - \boldsymbol{x}_0|^2 \right\}. \end{aligned} \tag{46}$$

This relation satisfies the free surface condition (42) under the assumption of two term expansions. In addition, substituting equation (46) to the kinematic condition equation (38), we obtain the following form:

$$\boldsymbol{n}\cdot\nabla\left\{ \frac{1}{2}|\boldsymbol{x}|^2 - \frac{1}{2}|\boldsymbol{x} - \boldsymbol{x}_0|^2 \right\} - \boldsymbol{n}\cdot\boldsymbol{x} = \boldsymbol{0} \quad \Leftrightarrow \quad \boldsymbol{n}\cdot(\boldsymbol{x} - \boldsymbol{x}_0) = \boldsymbol{0} \tag{47}$$

where $\boldsymbol{n}$ is the normal vector at $\boldsymbol{x}$. This means the free surface shape in the jet region, which is the straight line connecting $\boldsymbol{x}_0$ and $\boldsymbol{x}$.

The convergence of solutions are judged from the mass conservation rule. For similarity solutions, this can be expressed by the simple condition that two area S_1 and S_2 are equal, that is, $S_1 = S_2$. Finally, the hydrodynamic pressure can be computed by using:

$$\frac{p}{\rho V^2} = -\phi + \boldsymbol{x}\cdot\nabla\phi - \frac{1}{2}|\nabla\phi|^2 \tag{48}$$

4 Numerical results

In advance, we mention to the computational size dealt with in the present numerical study. As the radiation condition is not imposed, the side wall Γ_w are needed to be far away from the body to avoid the influence of the reflection from the boundary Γ_w. Only setting it to $x = 20.0m$ in Fig.1 and $x = 20.0$ in Fig.7, we can obtain practical solutions. The water depth is set to be $y = 6.0m$ and $y = 4.0$, respectively. In the numerical simulation, the computation is started initially submerged into water slightly, then the bottom is located at $y = -0.01m$. The total number of nodes is about 360 points, particularly, 30, 60 (initially 40), 250 and 20 are shared on Γ_c, Γ_B, Γ_F and Γ_W, respectively. On the free surface, the element size gradually becomes coarse as far from the body.

Considering the water impact of a wedge, the problem is solved by the nonlinear simulation method in the time domain and the iterative method for similarity solutions. We compared both results of the pressure distribution on the wedge with different deadrise angle α. These results are shown in Fig.9. We can recognize good agreement and specially the prediction in the jet region is acceptably stable. Corresponding results of the free surface profiles by the numerical simulation method are shown in Fig.10. Since we make the cut-off operation to the jet tip, the too much jet ejection is not observed, but the total length of the free surface is reduced to a certain extent.

Next we investigate the influence of the initial condition to the computation. It is demonstrated in Fig.11. Results of the left hand of the figure were obtained by using the initial condition (10). We can observe the formation of the convex on the free surface under the jet root just after the moment of water impact. Although the convexity of the free surface on the impact of a wedge was discussed by Mackie (1962), this is partly because the resolution of the computation near

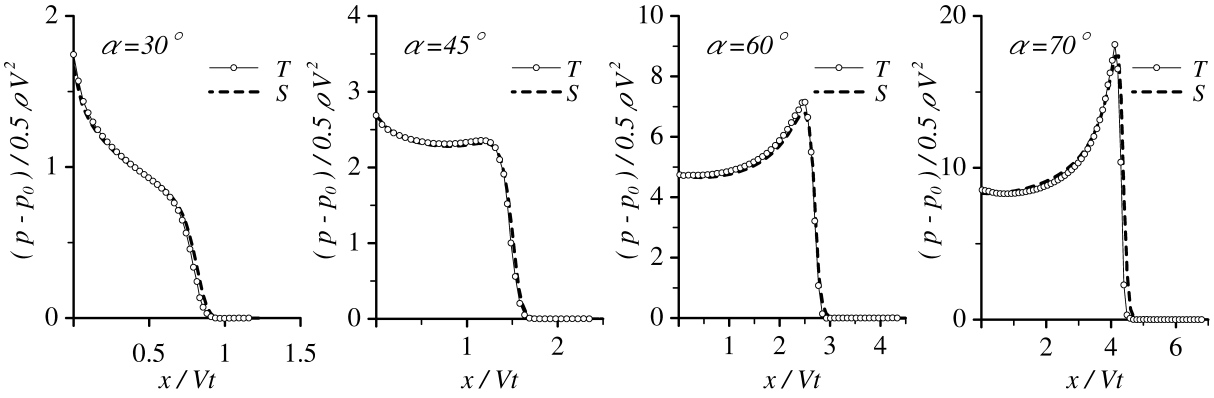

Fig. 9: The pressure distributions on the wedge in disregarding the gravity effect. (T: time domain solution, S: similarity solution)

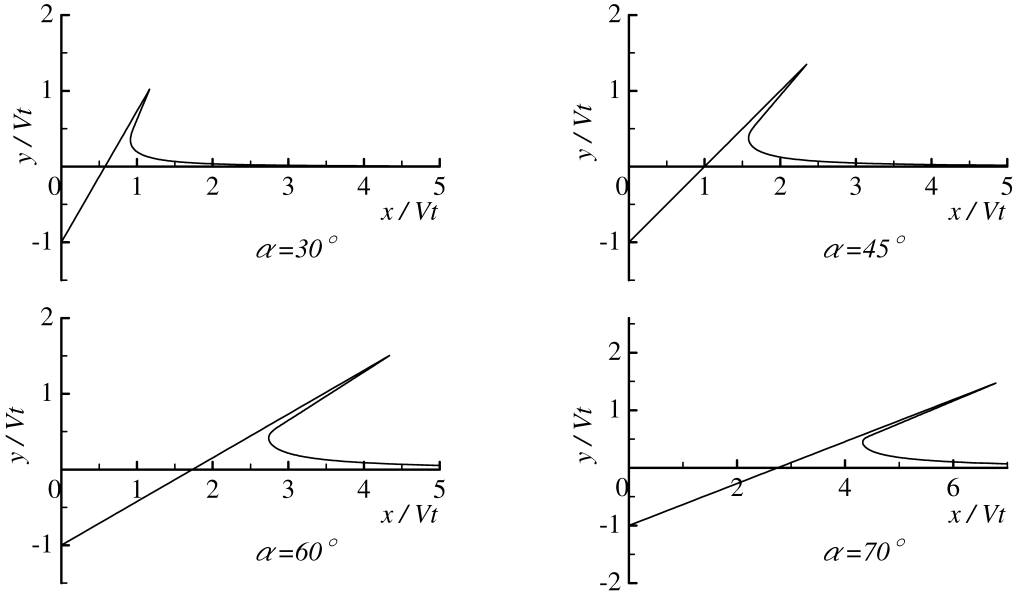

Fig. 10: The free surface profiles in disregarding the gravity effect.

the intersection is insufficient. Another reason is probably the lack of the consideration on the compressibility of the fluid as discussed by Korobkin (2004). The computed pressure indicates the small negative value and the high peaked value in the transient process to the steady value. On the other hand, the results of the right hand were obtained by taking account of the initial disturbance, particularly which was computed by the iterative computation in section . In these cases, such a convex are not observed and the peak value is also smaller. The influence of the initial condition should be taken into account in predicting the maximum pressure

Retaining the gravity term in the problem, we can simulate the evolution of the free surface from the jet formation up to the re-entry against the underlying free surface. Such computational results are shown in Fig.12 and Fig.13. So far the gravity effect has been always neglected in the water impact analysis based on the potential theory for the rational reason. The present numerical procedures hopefully enable the global simulation combining the hydrodynamic analysis with the free surface flow analysis. The adopted cut-off model doesn't disturb the evolution of the free surface as shown in Fig.5.

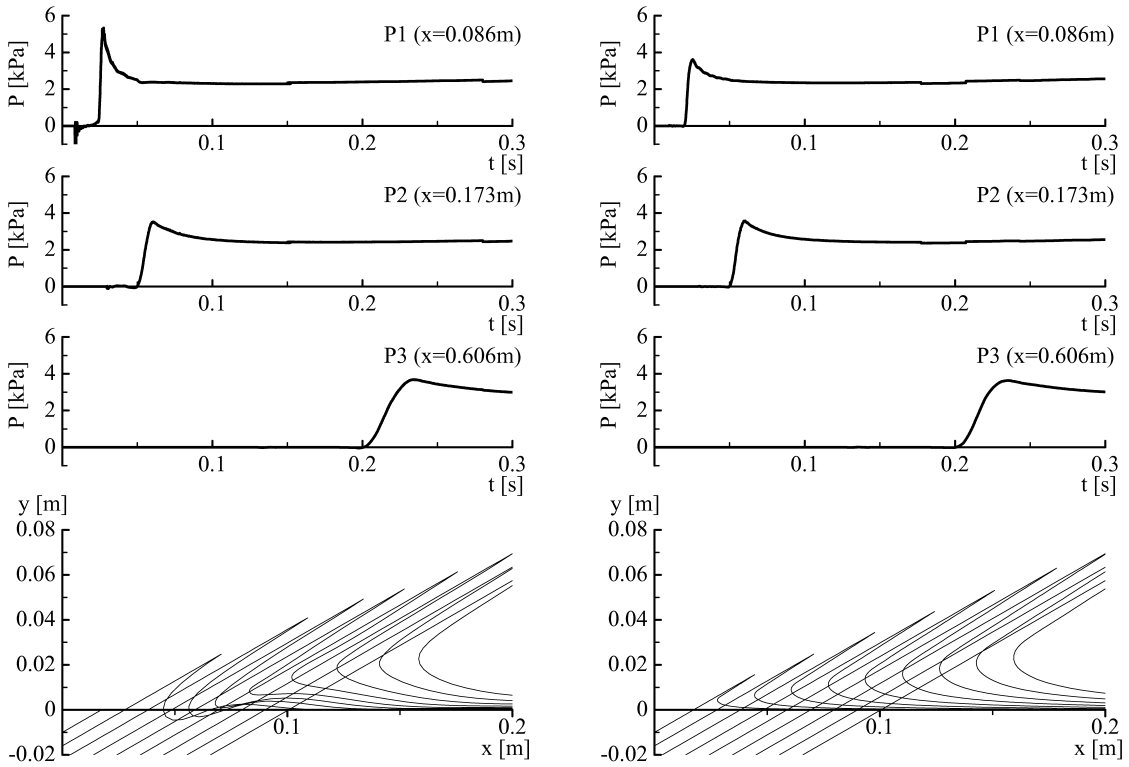

Fig. 11: Time histories of the pressure at fixed points on the wedge with $\alpha = 60°$ and $V = 1m/s$, and free surface profiles at an early stage of the impact, from 0.0s to 0.048s every 0.006s, are shown. Left figures are the computations without initial disturbance, and right ones are the computations with initial disturbance.

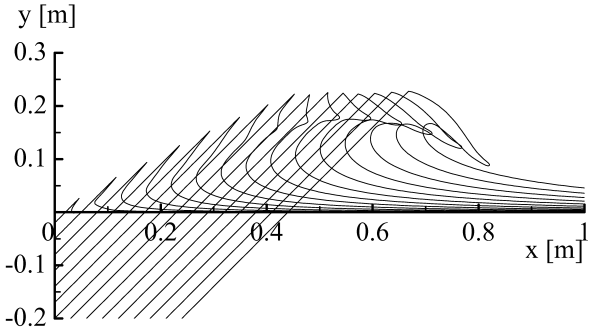

Fig. 12: Free surface evolution ($\alpha = 45°$).

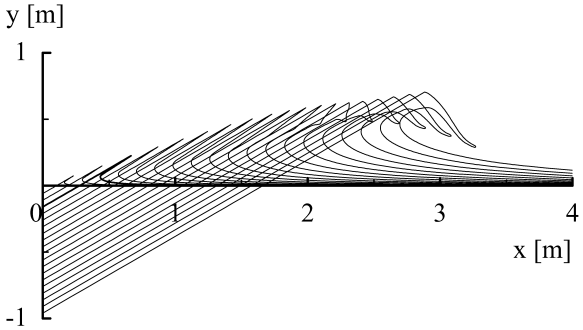

Fig. 13: Free surface evolution ($\alpha = 60°$).

5 Conclusions

Water impact problems for the wedge at the constant speed have been analyzed numerically in the frame of the potential flow assumption. The construction of numerical procedures in the time domain were intended to enable the global simulation combining the hydrodynamic analysis with the free surface flow analysis. For purposes of it, the computational model of the jet flow has been proposed and its availability was demonstrated for the wedge impact case. The iterative numerical procedure for similarity solutions was also studied to obtain the initial condition for the numerical procedure in the time domain. Both numerical methods can provide good agreement for similarity solutions. Related to the initial condition, its treatment

is significant particularly in predicting the hydrodynamic pressure.

6 References

ARMOND, J.-L.; COINTE, R. (1987), *Hydrodynamic impact analysis of a cylinder*, Jounal of Offshore and Mechanics and Arctic Engineering, ASME, Vol.9, pp.237-243.

BATTISTIN, D.; IAFRATI, A. (2003), *Hydrodynamic loads during water entry of two-dimensional and axisymmetric bodies*. Jounal of Fluid and Structures, Vol.17, pp.643-664.

BATTISTIN, D.; IAFRATI, A. (2004), *A numerical model for the jet generation by water impact*, Journal of Engineering Mathematics, Vol.48, pp.353-374.

CHAPMAN, S .J.; GILLOW, K. A.; HOWISON, S. D.; OCKENDON, J. R (1997), *Asymptotics of violent surface motion*, Philosophical Trans. of the Royal Soc. , Series A, Vol.355, pp.679-685.

COINTE, R.; GERYER, P.; KING, B.; MOLIN, B.; TRAMONI, M. (1990), *A nonlinear and linear motionsof a rectangular barge in a perfect fluid*, Proceedings of 18th Symp. on Naval Hydrodynamics, Ann Arbor, pp.85-99.

DOBROVOL'SKAYA, Z. N. (1969), *On some problems of similarity flow of flow with a free surface*, Jounal of Fluid Mechanics, Vol.36, pp.805-829.

FALTINSEN, O. M. (2002), *Water entry of a wedge with finite deadrise angle*, Jounal of Ship Research, Vol.46, No.1, March, pp.39-51.

FONTAINE, A.; COINTE, R. (1997), *A slender approach to nonlinear bow waves*, Philosophical Trans. of the Royal Soc. , Series A, Vol.335, pp.565-574.

GREENHOW, M. (1987), *Wedge entry into initial calm water*, Applied Ocean Research, Vol.9, No.4, pp.214-223.

HOWISON, S. D.; OCKENDON, J. R.; WILSON, S. K. (1991), *Incompressible water-entry problems at small deadrise angles*, Jounal of Fluid Mechanics, Vol.56, pp.173-192.

IAFRATI, A.; KOROBKIN, A. (2000), *Liquid flow close to intersection point*, Proceedings of 15th Intl. Workshop Water Waves and Floating Bodies.

IAFRATI, A.; KOROBKIN, A. A. (2002), *Hydrodynamic loads at the early stage of a floating wedge impact*, Proceedings of 17th Intl. Workshop Water Waves and Floating Bodies.

ISOPE NUMERICAL WAVE TANK GROUP (1999), *Report of the workshop of ISOPE Numerical Wave Tank Group*, http://www.isope.org/conferences/conferences.htm

KOROBKIN, A. A. (1996), *Water impact problem in ship hydrodynamics*, Ch.7 in Advance in Marine Hydrodynamics, M. Ohkusu, Ed., Computational Mechanics Publishing, Southampton, Boston.

KOROBKIN, A. A. (2004), *Jetting by floating wedge impact*, Proceedings of 19th Intl. Workshop Water Waves and Floating Bodies.

LIN, W. M.; NEWMAN, J. N.; Yue, D. K. (1984), *Nonlinear Forced Motions of Floating Bodies*, Proccedings of 15th Symposium on Naval Hydrodynamics, pp.33-49.

LU, C. H.; HE, Y. .S.; WU,G. X. (2000), *Coupled analysis of nonlinear interaction between fluid and structure during impact*. Jounal of Fluid and Structures, Vol.14, pp.127-146.

MACKIE, A. G. (1969), *The water entry problem*, Qurut. Journ.Mech. and Applied Math., Vol.22, pp.1-17.

MEI, X.; LIU, Y; YUE, D. K. P. (1999), *On the water impact of general two-dimensional sections*, Applied Ocean Research, Vol.21, pp.1-15.

OHTSUBO, H.; FUKUMURA, M. (1987), *Simplified analysis of impact pressure taking account of splash.*(in Japanese), Journal of the Society of Naval Architects of Japan, Vol.162, pp.374-380.

ROBERTS, A. J. (1987), *Transient Free-Surface Flows Generated by a Moving Vertical Plate*, Q. J. Mech. Appl. Math., Vol.40 pp.129-158.

TAKAGI, K.; NAITO, S. (1989), *An Application of Boundary Element Method to the Fluid-Body Interaction Problem*, Proccedings of 18th International conference on Offshore Mechanics and Arctic Engineering, pp.504-516.

TANIZAWA, K. (1985), *Self-similar solution of wedge entry problem by BEM* (in Japanese), Journal of the Kansai Society of Naval Architects, Japan, Vol.196, pp.147-154.

TANIZAWA, K. (1995), *A nonlinear simulation method of 3-D body motion in waves -1st report-*, Journal of the Society of Naval Architects of Japan, Vol.178, pp.179-191.

WAGNER, H. (1932), *Über Stoß- und Gleitvorgänge an der Oberfläche von Flüssigkeiten*, Zeitschr. für Angew. Math. und Mech., Vol.12, 4, pp.193-235.

WU, G. X.; EATOCK TAYLOR, R. (1990), *Transient motion of a floating body in steep water waves*, Proceedings of 11th Intl. Workshop Water Waves and Floating Bodies.

WU, G. X.; SUN, H.; HE, Y. S. (2004), *Numerical simulation and experimental study of water entry of a wedge in free fall motion*, Jounal of Fluid and Structures, Vol.19, pp.277-289.

YIM, B. (1985), *Numerical solution for two-dimensional wedge slamming with a nonlinear free-surface condition*, Proceedings of 4th International Conference on Numerical Ship Hydrodynamics, pp.107-116.

ZHAO, R.; FALTINSEN, O. (1993), *Water entry of two-dimensional bodies.* Jounal of Fluid Mechanics, Vol.246, pp.593-612.

ZHAO, R.; FALTINSEN, O.; AARSNES, J (1996), *Water entry of arbitrary two-dimensional sections with and without flow separation.* Proceedings of 21th Symp. on Naval Hydrodynamics, pp.408-423.